

# Features of Interference of Kummer Beams for Optical Measurement Problems

N. V. Shostka (Lyakhovich)<sup>a,\*</sup>, B. V. Sokolenko<sup>a</sup>,  
V. I. Voititskii<sup>a</sup>, and A. V. Prisyazhnyuk<sup>a</sup>

<sup>a</sup> Crimean Federal University, Simferopol, 295007 Russia

\*e-mail: nataliya\_shostka@mail.ru

Received February 17, 2022; revised March 22, 2022; accepted April 12, 2022

**Abstract**—An optical vortex interferometry model based on Kummer beams with an integer topological charge is presented. The proposed approach makes it possible to improve the stage of extracting data on the phase shift of the object beam introduced by an investigated object directly via detecting the angular positions of local minima of the intensity of a field of superposition of Kummer and Gaussian beams with different amplitude ratios.

**Keywords:** Kummer beam, interference, optical metrology

**DOI:** 10.1134/S1063785022040198

The use of light beams with a wave-front singularity (optical vortex) in various measuring systems is an active area in solving problems of optical metrology. The geometry of the wave front of a scalar optical vortex is a helicoid with a singularity on the axis in which the phase is not defined, which undergoes a jump that is multiple of  $2\pi$  when bypassing the singularity along a closed contour [1]. Such a wave structure exhibits a certain stability during beam propagation and has a characteristic intensity minimum in the vicinity of the singularity, which is a kind of marker for the vortex position and can be determined with high accuracy [2]. In recent years, optical vortex beams have been used to measure various physical quantities, including the refractive index, thickness, relief height, and surface roughness [3–5]. The approaches of the interference analysis of vortex beams underlying the optical topography ensure the nondestructive, fast, and accurate control of optically smooth surfaces. This makes it possible to use the advantages of singular beams, specifically, (i) the wave-front helicity, which gives a more noticeable response to the optical path difference changes, (ii) isolation of field zeros as a point probe when scanning the test sample [6], and (iii) circular symmetry, the change of which reflects the state of the diffracted optical field upon detection of microscopic phase inhomogeneities [7].

In practice, the interference analysis of a wave front screw dislocation can be divided into two main approaches: (i) the scenario of axial superposition with a reference beam having a strongly pronounced spherical wave front and (ii) the interference with an oblique plane wave. Depending on the chosen scenario, the

interference pattern takes the form of a spiral or lines of equal slope with a bifurcation area (“fork”). Computer analysis of such interferograms allows one to extract information about the phase delay of the object beam introduced by an investigated specimen.

In this work, we propose an approach based on the axial interference of a singular beam and a reference beam with a smooth wave front. Such a superposition mode eliminates the degeneracy of the axial zero in the intensity distribution, which makes it possible to extract the value of the difference of the optical-beam path directly from its profile by tracking the change in the angular position of local intensity zeros and to determine the phase shift introduced in the object beam.

The complex amplitude of the vortex beam field can be described by the confluent Kummer hypergeometric function, due to which such light fields are called “Kummer beams” [8]. This family of functions is an exact solution of the Helmholtz parabolic equation and the numerical simulation based on them corresponds qualitatively to experimental observations. The Kummer beam axis contains a degenerate intensity of zero, in the vicinity of which the phase has incursion  $2\pi/l$ , where  $l$  is the vortex topological charge, which takes integer values [9].

In the paraxial approximation, the complex amplitude of the electric field of the vortex beam in the cross section will be described by the equation  $E_V(r, \varphi, z_V) = \eta \tilde{E}_V(r, \varphi, z_V) \exp(-ikz_V)$ , where  $(r, \varphi, z_V)$  are the cylindrical coordinates,  $t = 0, 1, \dots, l - 1$ ,  $z_V$  is the optical-path length in the propagation direction,  $k = 2\pi/\lambda$  is

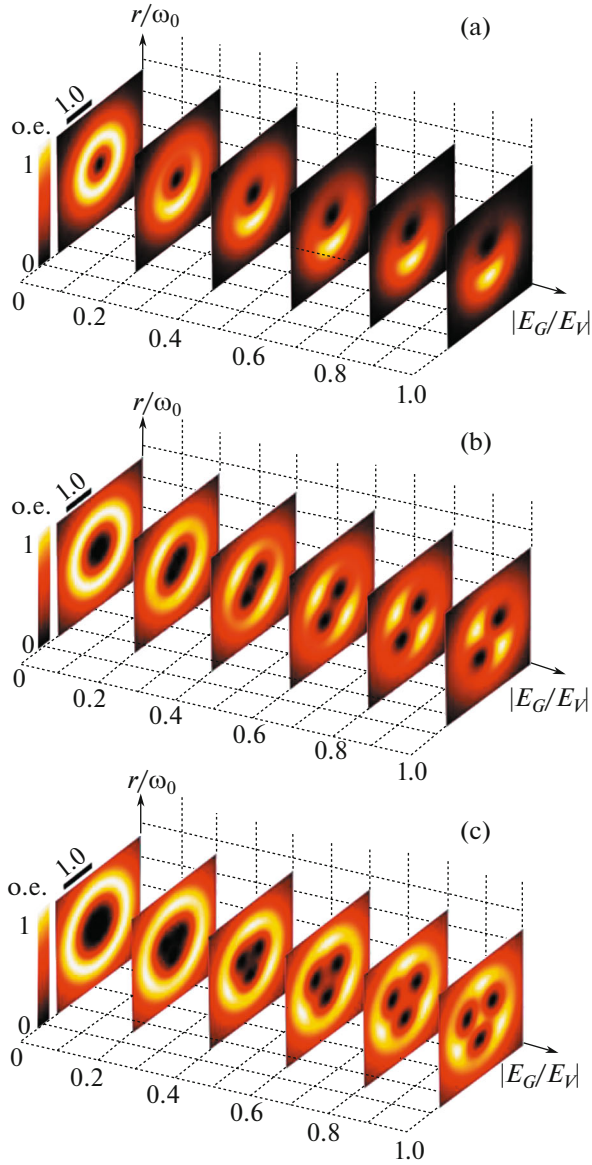


**Fig. 1.** Transverse intensity distributions of the interference field of Gaussian and Kummer beams with topological charges of  $l =$  (a) 1, (b) 2, and (c) 3 as functions of the amplitude ratio  $|E_G/E_V|$ . The simulation parameters are  $\omega_{0,G} = 180 \mu\text{m}$ ,  $z_V = 198 \text{ mm}$ , and  $z_G = 228 \text{ mm}$ .

the wavenumber, and  $\eta$  is the parameter normalizing to unity the maximum complex amplitude  $\tilde{E}_V(r, \varphi, z_V)$ , the form of which in the far diffraction zone can be written as [10]

$$\tilde{E}_V(r, \varphi, z_V) = \frac{(-i)^{|l|+1}}{2\pi l!} \left(\frac{z_r}{z_V}\right) \Gamma\left(\frac{|l|+2}{2}\right) \exp\left(\frac{ikr^2}{2z_V} + il\varphi\right) \times \left(\frac{k\omega_0}{\sqrt{2z_V}} r\right)^{|l|} {}_1F_1\left[\frac{|l|+2}{2}, |l|+1, -\left(\frac{k\omega_0}{\sqrt{2z_V}} r\right)^2\right], \quad (1)$$

where  $z_r = k\omega_0^2/2$  is the Rayleigh length,  $\omega_0$  is the initial beam waist radius,  $\Gamma(\chi)$  is the  $\gamma$  function, and  ${}_1F_1(\alpha, b, \zeta)$  is the Kummer hypergeometric function.

The most widespread scenario is the interference of a vortex beam and a Gaussian beam, the complex amplitude of which can be expressed accurate to the normalizing factor as

$$E_G(r, z_G) = A_G \exp\left[-\frac{r^2}{\omega_G^2(z_G)}\right] \times \exp\left[\frac{ikr^2}{2z_G[1+(z_{rG}/z_G)^2]} - ikz_G\right], \quad (2)$$

where  $A_G$  is the amplitude parameter,  $\omega_G(z_G) = \omega_{0G}\sqrt{1+(z_G^2/z_{rG}^2)}$ ,  $z_{rG} = k\omega_{0G}^2/2$  is the Rayleigh length,  $\omega_{0G}$  is the Gaussian-beam waist radius in the initial plane  $z = 0$ , and  $z_G$  is the optical path length. The resulting distribution of the intensity of the field of interfering waves  $E_V(r, \varphi, z_V)$  and  $E_G(r, z_G)$  is described by the well-known equation

$$I(r, \varphi, z_G, z_V) = |E_V|^2 + |E_G|^2 + (E_V E_G^*) + (E_V^* E_G), \quad (3)$$

where  $(*)$  is the complex conjugation sign.

Let us follow the changes in the intensity of the interference field upon variation in the optical-path difference controlled by the conditional delay line and the ratio between the integral beam intensities. The parameter of the optical path difference in free space (the refractive index of a medium is the same for both beams and can be taken as unity) takes into account the difference between geometric paths of the beams; this allows one to estimate the sensitivity of the interference pattern to their change.

The first analyzed parameter is the effect of the field amplitude ratio on the interference pattern. In the investigated case, upon variation in the ratio between amplitudes of the vortex and Gaussian beams ( $0 < |E_G/E_V| \leq 1$ ), degeneracy of the axial singularity is eliminated. As a result of the structural instability of a higher-order vortex beam ( $|l| > 1$ ),  $l$  independent optical vortices appear in the field distribution, the topological charge of which is unity and has the same sign. A similar evolution of the interference pattern was demonstrated by Dennis for the Laguerre–Gaussian beams [11]. The shift of vortices and, consequently, field zeros from the axis ( $r = 0$ ) is proportional to the amplitude ratio of the Gaussian and Kummer beams:  $\rho \propto \sqrt[|l|]{|E_G/E_V|}$ . The type of splitting of the intensity zeros takes the form of an equilateral  $l$ -gon with the center on the vortex beam axis and intensity zeros in the vertices (Figs. 1a–1c). The formed vortex structure is preserved during propagation in free space due to the proportionality of the beam transverse dimensions in the interferometer arms and curvatures of their wavefronts up to the scaling transformations

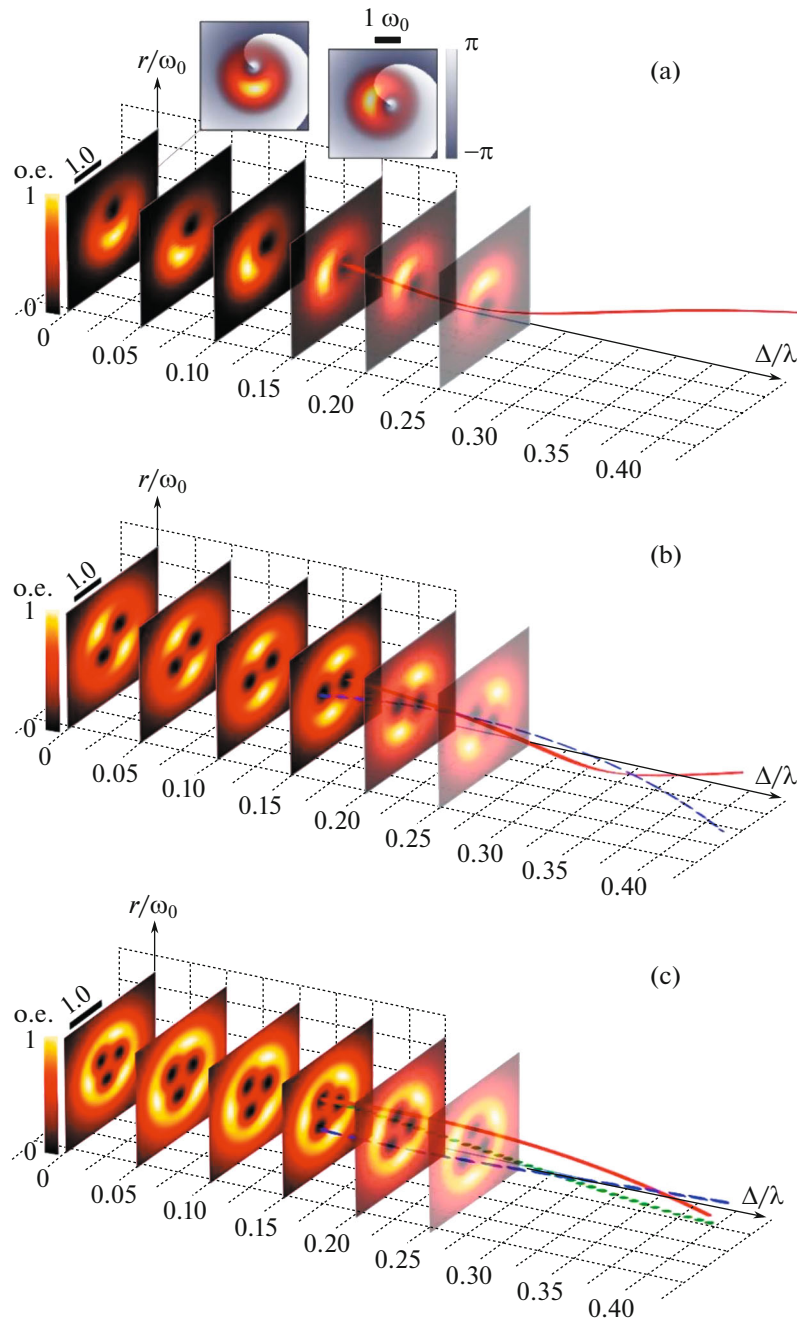


**Fig. 2.** Calculated patterns of the evolution of the transverse intensity distribution of the superposition of Gaussian and Kummer beams with topological charges of  $l =$  (a) 1, (b) 2, and (c) 3 upon variation in geometric-path difference  $\Delta$  between the beams. The solid line shows a fragment of the trajectory of the vortex with the index  $t = 0$ ; the dashed line, of the vortex with the index  $t = 1$ ; and the dotted line, of the vortex with the index  $t = 2$ . The simulation parameters are  $\omega_{0,G} = 180 \mu\text{m}$ ,  $z_V = 198 \text{ mm}$ ,  $z_G = 228 \text{ mm}$ , and  $|E_G/E_V| = 0.75$ .

caused by the beam divergence. We note that the Kummer beams retain self-similarity in the far diffraction zone; therefore, the difference between the interferometer arm lengths did not exceed the Rayleigh length and the simulation parameters were close to experimentally implementable. This opens up the

opportunity for the obtained optical structure to be used as a probe beam with experimentally detected positions of the isolated field zeros.

The second dependence, which determines the resolution of this approach in metrological problems, can be obtained using the characteristics of the field

spatial dynamics at different delay line lengths  $\Delta = (z_G - z_V)/2$  (Figs. 2a–2c). For the three presented absolute values of the topological charge, each of the field local zeros moves along a spiral trajectory during the growth of the delay line length. This trajectory type is determined by a fundamental property of the Kummer beam: a helicoidal wave front [6]. The presented superposition of the intensity of the resulting field and its phase portrait (Fig. 2a) is indicative of the exact correspondence between the phase singularity position and the amplitude zero. We note that all the resulting fields are invariant under rotation by the angle  $2\pi/l$ , as a result of which the angular coordinate of the trajectory of each intensity zero is described as  $\theta_t = (\pi + k\Delta + 2\pi t)/l$ , where  $t$  corresponds to the number of the intensity zero and takes the values  $t = 0, 1, \dots, l - 1$ . The superposition with the Kummer beam with a unit topological charge will have the highest resolution. The change in the delay line from 0 to  $\lambda$  causes two complete rotations of the intensity zero in the field cross section. At the detection of a change in angle  $\theta$  accurate to 0.035 rad, the resolution will be  $\sim \lambda/180$ . Nevertheless, in practice, the second reference point can increase the accuracy of determining the rotation angle, which does not exclude the use of the Kummer beam with a double topological charge.

The advantage of the proposed approach lies in the possibility of real-time automatic express processing of the beam superposition field. Tracking the positions of zero intensity using neural networks and machine learning [2] without image preprocessing will significantly speed up the extraction of data on the path difference. It is promising to move from matrix screening of the entire beam field to single-pixel detectors, the signal of which can be transmitted faster and with a larger capacity.

#### FUNDING

This study was supported by the Russian Science Foundation, project no. 20-72-00065.

#### CONFLICT OF INTEREST

The authors declare that they have no conflicts of interest.

#### REFERENCES

1. H. Rubinsztein-Dunlop, A. Forbes, M. R. Dennis, and M. V. Berry, *J. Opt.* **19**, 1 (2017). <https://doi.org/10.1088/2040-8978/19/1/013001>
2. A. Popiołek-Masajada, E. Frączek, and E. Burnecka, *Metrol. Meas. Syst.* **28**, 497 (2021). <https://doi.org/10.24425/mms.2021.137131>
3. Y. Na and D. K. Ko, *Opt. Laser Technol.* **112**, 479 (2019). <https://doi.org/10.1016/j.optlastec.2018.11.053>
4. B. V. Sokolenko and D. A. Poletaev, *Proc. of SPIE* **10350**, 1035012 (2017). <https://doi.org/10.1117/12.2273395>
5. P. Schovánek, P. Bouchal, and Z. O. Bouchal, *Opt. Lett.* **45**, 4468 (2020). <https://doi.org/10.1364/OL.39207>
6. B. Sokolenko, N. Shostka, O. Karakchieva, A. V. Volyar, and D. Poletaev, *Comput. Opt.* **43**, 741 (2019). <https://doi.org/10.18287/2412-6179-2019-43-5-741-746>
7. A. Bekshaev, A. Khoroshun, and L. Mikhaylovskaya, *J. Opt.* **21**, 084003 (2019). <https://doi.org/10.1088/2040-8986/ab2c5b>
8. A. Bekshaev, A. Khoroshun, J. Masajada, and A. V. Chernykh, *J. Opt.* **23**, 034002 (2021). <https://doi.org/10.1088/2040-8986/abcea7>
9. V. V. Kotlyar, A. A. Kovalev, and E. G. Abramochkin, *Comput. Opt.* **43**, 735 (2019). <https://doi.org/10.18287/2412-6179-2019-43-5-735-740>
10. V. V. Kotlyar and A. A. Kovalev, *J. Opt. Soc. Am. A* **25**, 262 (2008). <https://doi.org/10.1364/JOSAA.25.000262>
11. M. R. Dennis, *Opt. Lett.* **31**, 1325 (2006). <https://doi.org/10.1364/OL.31.001325>

*Translated by E. Bondareva*